ELSEVIER

Biochemical Pharmacology 63 (2002) 1979–1988

Biochemical Pharmacology

Characterization of F-actin depolymerization as a major toxic event induced by pectenotoxin-6 in neuroblastoma cells

Francisco Leira[a,*], Ana G. Cabado[a], Mercedes R. Vieytes[b], Yolanda Roman[c], Amparo Alfonso[c], Luis M. Botana[c], Takeshi Yasumoto[d], Claudia Malaguti[e], Gian P. Rossini[e]

[a]*ANFACO-CECOPESCA, Campus Universitario de Vigo, 36310 Vigo, Spain*
[b]*Dpto. de Fisiología Animal, Facultad de Veterinaria de Lugo, 27002 Lugo, Spain*
[c]*Dpto. de Farmacología, Facultad de Veterinaria de Lugo, 27002 Lugo, Spain*
[d]*Japan Food Research Laboratories, Tama Laboratories, 6-11-10 Nagayama, Tama, Tokyo 206-0025, Japan*
[e]*Dpto. di Scienze Biomediche, Universitá di Modena e Reggio Emilia, Via Campi 287, I-41100 Modena, Italy*

Received 22 January 2002; accepted 6 March 2002

Abstract

Pectenotoxins are a group of marine toxins produced by dinoflagellates and formerly included within the group of diarrhetic shellfish poison or toxins (DSP or DST) because of their physico-chemical properties. However, toxicological data on pectenotoxins are still very scarce and its mechanism of action is largely unknown, but toxicity in laboratory animals has been demonstrated by intraperitoneal injection. In this report, we present results of *in vitro* toxicological assessment of pectenotoxin-6, a derivative of the parental toxin pectenotoxin-2 first isolated from toxic scallops. Results obtained demonstrate an specific time- and dose-dependent depolymerization of F-actin in neuroblastoma cells exposed to pectenotoxin-6 (half-maximal effect about 700 nM at 24 hr). The change in the state of polymerization of actin was not accompanied by other major effects on specific signal transduction pathways or cell survival rate. Pectenotoxin-6 does not modify cytosolic calcium levels either in a calcium containing or calcium-free medium in human lymphocytes. Only when capacitative calcium influx was first activated, the toxin addition significantly decreased the following calcium influx. In these cells, pectenotoxin-6 only modifies cAMP (adenosine 3′,5′-cyclic monophosphate) levels in calcium-free conditions. In addition, no effect on cell attachment or apoptosis induction was observed at micromolar concentrations of pectenotoxin-6. Therefore, we conclude that cytoskeletal disruption is a key mechanism of PTX6-induced toxicity in eukaryotic cells.

Keywords: Pectenotoxin-6; Cytotoxicity; F-actin; G-actin; Neuroblastoma; Apoptosis

1. Introduction

Pectenotoxins (PTXs) are a group of cyclic polyether macrolide compounds from marine origin first isolated from toxic shellfish by Yasumoto *et al.* [1]. PTXs have been classically included within DSP (diarrhetic shellfish poison) because of their phytoplanktonic origin and lipophilic nature, thus, being co-extracted with diarrhogenic toxins (okadaic acid, dinophysistoxins) from contaminated shellfish. Actually, eight different PTXs (PTX1 to 7 and PTX10) [2] and two new derivatives of PTX2 (PTX2 seco-acid and 7-epi-PTX2 seco-acid) [3] have been described and characterized mainly in shellfish. PTX2 is suspected to be the precursor toxin of the whole PTXs through biotransformation processes which take place in the digestive glands of bivalves.

During last years, PTXs have been isolated from shellfish of different culture areas in Europe, Asia and Oceania [4–6], thus, raising an increasing concern in Public Health authorities. In addition, a debate on the convenience of keeping PTXs within DSP has began since PTXs do not inhibit protein phosphatases nor induce diarrhea in mammals [7,8]. However, toxicological data are very scarce and further studies on the effects of PTXs are urgently required.

* Corresponding author. Tel.: +34-986469303; fax: +34-986469269.
E-mail address: fleira@anfaco.es (F. Leira).

Abbreviations: DSP, diarrhetic shellfish poison; PTXs, pectenotoxins; PTX6, pectenotoxin-6; PTX1, pectenotoxin-1; PTX2, pectenotoxin-2; EDTA, ethylenediaminetetracetic acid; SDS–PAGE, sodium dodecyl sulfate–polyacrilamide gel electrophoresis; PBS, phosphate buffered saline; cAMP, adenosine 3′,5′-cyclic monophosphate.

0006-2952/02/$ – see front matter
PII: S0006-2952(02)00993-0

Most toxicological data available on PTXs (both *in vivo* and *in vitro*) have been obtained with PTX1, showing liver damage following intraperitoneal injection in mice [8] and morphological changes in freshly prepared hepatocytes [9,10]. In addition, LD_{50} values in mice have been obtained for most PTXs, revealing the highest lethality for PTX2 [3,11], which further supports the hypothesis of PTX2 as the parental compound of PTX group. Thus, successive oxidation of substituent in C18 in the digestive glands of bivalves would diminish the toxicity of PTXs. Additional data obtained with PTX1 showed no antibacterial or antifungal activity for this toxin [12], although its physicochemical structure is similar to that of the polyether macrolide goniodomin A, a highly potent antifungal compound. PTX2 has been proven to induce lethality of brine shrimp (*Artemia salina*), as well as cytotoxic activity against several human cell lines, although significant differences were observed in the relative LC_{50} values obtained for each of them [13].

Apoptosis induction by PTXs has already been studied since apoptosis or programmed cell death is a common event in cells exposed to lipophilic phycotoxins [14–19]. Primary cultures of rat and salmon hepatocytes exposed to PTX1 in the micromolar range showed rapid apoptotic changes [20], but no further studies concerning apoptotic activity of PTXs have been carried out in human cells. No additional data are available on acute and chronic effects of PTXs, and the mechanism of action of these toxins is currently unknown.

In this work, we present results obtained on *in vitro* toxicological evaluation of PTX6, an acidic PTX isolated from toxic scallops [11]. A wide array of morphological and biochemical indicators of toxicity have been assessed in different eukaryotic cells in order to obtain relevant information on the mechanism of action of PTX6. Key experiments have been confined to the most relevant cell lines due to the tiny amounts of pure toxin available. We demonstrate that PTX6 induces an specific time- and dose-dependent depolymerization of F-actin in neuroblastoma cells exposed to micromolar concentrations of PTX6. The change in the state of polymerization of actin was not accompanied by other major effects on specific signal transduction pathways or cell survival rate, thus, suggesting that cytoskeletal disruption is a key mechanism of PTX6-induced toxicity.

2. Materials and methods

2.1. Materials

Peroxydase-linked anti-rabbit Ig antibodies, and the enhanced chemiluminescence (ECL) detection reagents were from Amersham Biosciences. Prestained molecular mass markers, and monoclonal anti-actin antibody from mouse were obtained from Sigma. The nitrocellulose membrane Protran B83 was obtained from Schleicher & Schuell. Thapsigargin, ionomycin and forskolin were from Alexis Corporation. FURA-2 AM, FlCRhR (recombinant fluorescein-and rhodamine-labeled protein kinase A) and Influx™ Pinocytic Cell-Loading Reagent were from Molecular Probes. Ethilen-glicol-bis(β-aminoethylether) *N*,*N*,*N*′,*N*′-tetracetic acid (EGTA) and ethylenediaminetetracetic acid (EDTA), were from Sigma. Percoll® was from Pharmacia. The purification of PTX6 has been carried out as previously described [21], and the purity of the compound was confirmed by high performance liquid chromatography and spectral data [22]. All other reagents were of analytical grade.

2.2. Cell culture

Neuroblastoma cell line BE(2)-M17 (ATCC Number CRL-2267) was purchased from the European Collection of Cell Cultures and seeded in 25 cm^2 flasks at a seeding density of 4×10^4 cells/cm^2. Cells were cultured on Earle's modified Eagle's medium (EMEM): Ham's F12 (1:1) with 2 mM glutamine, 1% non-essential amino acids, 15% fetal bovine serum, 50 mg/L gentamycin and 50 μg/L amphotericine B (Biochrom KG) at 37°/5% CO_2 until 70–90% confluence was reached. For microplate assays, the cells were seeded in 96-well microtiter plates at a density of 2500 cells/well. Following an additional incubation of 48 hr, cells grown in microtiter plates were used for fluorimetric microplate assays.

HeLa S_3 cells were grown as small clumps attached to Petri dishes (90 mm diameter) in 5% carbon dioxide in air at 37°, with a culture medium composed of RPMI (Roswell Park Memorial Institute) 1640, containing 5% fetal calf serum, as previously described [19]. MCF-7 cells were grown in 5% carbon dioxide in air at 37°, in 90 mm diameter Petri dishes, with a culture medium composed of Dulbecco's modified Eagle medium, containing 1% nonessential amino acids and 10% fetal calf serum, as previously described [19].

2.3. F-actin assay

Quantitative analysis of F-actin pools was carried out as previously described [23] using Oregon Green®514-Phalloidin (Molecular Probes Inc.) to label F-actin. Triplicate analysis of F-actin levels were done in cells exposed for 1, 6, 24 and 48 hr to 1–10^4 nM PTX6.

2.4. Cell proliferation/cell attachment

The effect of PTX6 on cell proliferation was evaluated in triplicate with the CyQuant®Cell proliferation assay kit (Molecular Probes Inc.) as previously described [18]. Cells were incubated for 1, 24 and 48 hr with 1–10^4 nM PTX6 and then centrifuged (3900 rpm/5 min) to prevent a possible effect of cell detachment in the assay. Attachment of

cells to the ECM was evaluated using the same procedure in cells incubated for 24 hr with PTX6 in triplicate experiments, but avoiding the centrifugation step in order to remove non-adherent cells from the plate.

2.5. Mitochondrial membrane potential

Changes in mitochondrial membrane potential were evaluated with the mitochondria-selective fluorescent probe MitoTracker®Red-CMXRos (Molecular Probes Inc.). The procedure used was exactly as previously described [18] and results were expressed as percentage of values corresponding to controls of triplicate experiments in cells exposed for 1–48 hr to 1–10^4 nM PTX6.

2.6. Fractionation of proteins by sodium dodecyl sulfate–polyacrylamide gel electrophoresis and immunoblotting (SDS–PAGE)

Cells were washed three times with 20 mM PBS, and lysed by addition of 20 mM Tris–HCl, pH 7.5 at 2°, 1 mM EDTA and 2% SDS. Cytosoluble extracts were then obtained by centrifugation for 30 min at 16,000 *g*. The supernatants of this centrifugation were used for colorimetric determinations of protein content, with bicinchoninic acid [24], and then brought to 2% SDS and 5% β-mercaptoethanol, to be used for fractionation by SDS–PAGE.

Samples containing the same amounts of protein were fractionated by SDS–PAGE, according to Laemmli [25], using 10% separating gels and a 3% stacking gel. After completion of electrophoresis, proteins were electrophoretically transferred onto a nitrocellulose membrane (Protran B83), and binding sites remaining on the membrane were blocked by incubation of blots for 1 hr at room temperature with 20 mM Tris–HCl, pH 7.5 at 25°, 0.15 M NaCl, and 0.05% (v/v) Tween 20 (immunoblotting buffer) containing 3% non-fat dry milk. Membranes were then incubated for 1 hr at room temperature with immunoblotting buffer containing 1% non-fat dry milk and anti-actin antibody at a final 1:250 dilution. After incubation, membranes were washed five times with immunoblotting buffer, and incubated for 1 hr at room temperature with a peroxydase-linked secondary antibody at a 1:3000 dilution in immunoblotting buffer containing 1% non-fat dry milk. After washing, the membrane was developed by the ECL detection system.

2.7. Fluorescent labeling of actin

Selective labeling of F- and G-actin was carried out in cells grown on glass culture slides at 60–70% confluence. Cells were washed with prewarmed PBS (Sigma–Aldrich) pH 7.4 and then fixed for 15 min in 3.7% formaldehyde solution (Sigma–Aldrich) in PBS. After washing twice with PBS, cells were permeabilized for 15 min with 0.1% Triton®X-100 (Sigma–Aldrich) in PBS and then washed once with PBS. Fixed cells were pre-incubated with 1% bovine serum albumin (RIA grade, Sigma–Aldrich) in PBS for 30 min to reduce non-specific staining, and then F-/G-actin were specifically labeled with Oregon Green®514-phalloidin and Texas Red-DNAse I (Molecular Probes Inc.) by incubating for 30 min in the dark at room temperature. Finally, the slides were washed twice with PBS and coverslips were mounted with 10 μL mounting media and sealed with nail polish. Specimens were observed in a confocal Nikon Eclipse 800 microscope equipped with Ar:Kr laser, MRC-1024 software (Bio-Rad), Plan Apo 40/Plan Apo 60 objectives and an epifluorescence module with B2A/G2A filters.

2.8. Human lymphocytes isolation

The effect of PTX6 on cytosolic calcium and cAMP levels was evaluated in human lymphocytes in order to obtain information pertaining to healthy donors, which is more useful than that obtained in neoplastic cells. Peripheral human lymphocytes were isolated from heparinized blood extracted from healthy donors diluted 1:1 with PBS plus EDTA 2 mM by centrifugation through 57.5% isotonic percoll. Percoll was eliminated by washing three times with PBS plus EDTA 2 mM at 400 *g* for 5 min. Lymphocytes purity was always higher than 80%.

2.9. Measurement of cytosolic free calcium: image processing

Purified lymphocytes were loaded with Fura-2 AM (2 μM) for 10 min at 37°. Loaded cells were washed three times (400 *g*/2 min) and allowed to attach to poly-L-lysine-coated 22-mm glass coverslips for 10 min. The glass coverslips were inserted into a thermostated chamber (IntraCell) and cells were viewed with a Nikon Diaphot 200 microscope equipped with epifluorescence optics (Nikon 40X-immersion UV-Fluor objective). The light source was a 175 W xenon lamp, and light reached the objective with optic fiber. The chamber was used in the open bath configuration and additions made by aspiration and addition of fresh bathing solution. Intracellular calcium concentration was obtained from the images collected by dual excitation fluorescence, 340, 380 and 505 nm fluorescence emission for FURA with a Life Science Resource equipment. Intracellular calcium was calculated by using the method of Grynkiewicz *et al.* [26].

2.10. Measurement of intracellular cAMP levels: image processing

Purified lymphocytes were loaded with FlCRhR by the following protocol: 10 μL of Hypertonic Loading Medium (Influx™ pinocytic cell-Loading Reagent) containing 0.4 μL of FlCRhR were added to 300,000 purified

lymphocytes. After gently suspension the cells were incubated for 10 min at 37°. Then 3 mL of hypotonic lysis medium (water diluted saline solution (6:4)) were added and incubated for 1.5 min at 37°. Loaded cells were quickly washed three times (400 *g*/2 min) with saline solution and allowed to attach to poly-L-lysine-coated 22-mm glass coverslips for 10 min. The glass coverslips were inserted into the thermostated chamber (IntraCell) and cells were viewed with the microscope described in cytosolic calcium experiments. For FlCRhR the excitation wavelength was 490 and the emission 530 and 580 nm. FlCRhR is a single-excitation dual-emission dye, similar to native protein kinase A, whose emission spectrum changes with cAMP binding. In this way, the FlCRhR 530/580 emission ratio increases upon intracellular free cAMP concentration elevation [27]. Dibutyryl cAMP (dbcAMP) (200 μM) was added at the end of each experiment to test cAMP fluorosensor functionality.

2.11. Statistical analysis

All the experiments were done in triplicate and results were analyzed using the Student's *t*-test for unpaired data followed by pair-wise comparisons using the Mann–Whitney *U*-test. A probability level of 0.05 was used for statistical significance.

3. Results

3.1. Effect of PTX6 on F-actin cytoskeleton

Changes on F-actin have been evaluated since it is known that the actin cytoskeleton is targeted by several marine natural compounds including PTX2 [28]. As expected, neuroblastoma cells showed rapid morphological changes in response to PTX6. Results obtained by fluorimetric microplate assay (Fig. 1) demonstrated a time- and dose-dependent disruption of F-actin cytoskeleton in BE(2)-M17 cells exposed to PTX6 for 1–48 hr (half-maximal effect about 700 nM at 24 hr). Significant differences with controls were obtained in all cases at concentrations higher than 1 μM, and complete depolymerization of F-actin was observed after 6 hr incubation with 10 μM PTX6. Interestingly, these changes on F-actin cytoskeleton did not affect the attachment of cells to the extracellular matrix (ECM) as determined by fluorimetric microplate assay. As shown in Fig. 2, no cell detachment was observed at PTX6 concentrations inducing a complete disruption of F-actin structure in the cells.

In spite of decreased F-actin levels observed in response to PTX6, the total amount of actin remained unchanged in the cells, such as demonstrated by Western blot analysis of crude cytosolic extracts obtained from PTX6-treated and control cells (Fig. 3). Indeed, fluorimetric labeling revealed the loss of F-actin but increased G-actin staining in PTX6-

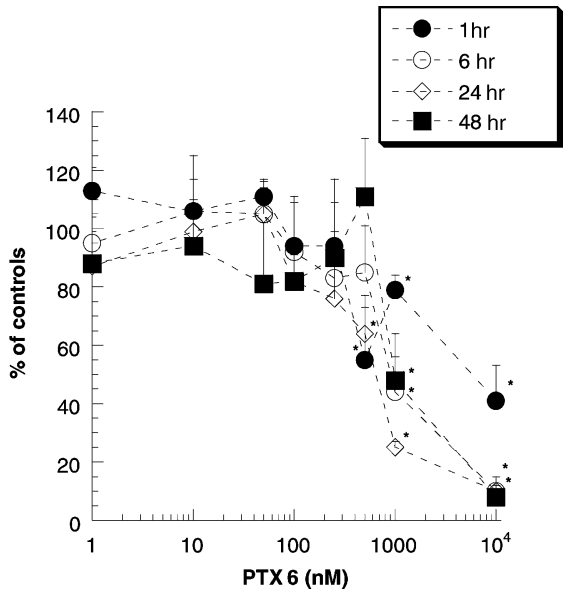

Fig. 1. Fluorimetric microplate analysis of F-actin levels in BE(2)-M17 cells incubated for 1–48 hr with 1–10^4 nM PTX6 (average ± SD; N = 3). Results are expressed as percentage of Oregon Green® 514-Phalloidin relative fluorescence with respect to control (untreated) cells. $^*P < 0.05$.

treated cells when compared to controls (Fig. 4A–D). These results further suggest an effect of PTX6 on the polymerization state of actin rather than a change affecting the protein itself. In addition, Western blot analysis of PTX6-treated MCF-7 and HeLa cells did not either show significant changes in the total amount of actin (data not shown).

3.2. Evaluation of apoptotic activity

The ability of PTX6 to induce apoptosis *in vitro* was evaluated by measuring changes in mitochondrial membrane potential, which is a common event in the apoptotic process induced by many different xenobiotics [29,30]. As shown in Fig. 5, PTX6 does not induce the collapse of mitochondrial membrane potential characteristic of apoptotic cells through the whole range tested (1–48 hr), thus likely indicating that apoptosis is not the major mechanism of PTX6-mediated toxicity. Therefore, apoptogenic activity of PTX6 could not be demonstrated in BE(2)-M17 cells at concentrations ranging from 1 nM to 10 μM, not showing significant differences in the values for mitochondrial membrane potential when compared to controls.

3.3. Effect on cell proliferation

The effect of PTX6 on cell proliferation was evaluated by fluorimetric microplate analysis of total DNA content in cells exposed for 1–48 hr at 1–10^4 nM PTX6. Results obtained in BE(2)-M17 cells did not significantly differ from controls (Fig. 6), thus indicating a negligible effect of PTX6 on cell proliferation. Similar results were obtained for HeLa and MCF-7 cells cultured in larger volumes,

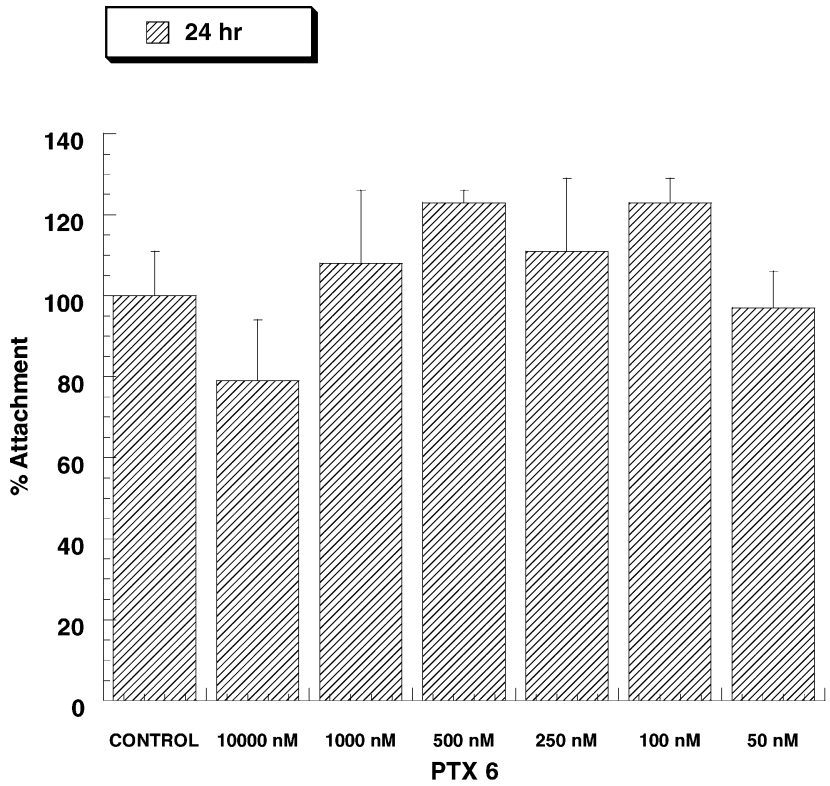

Fig. 2. Results of the cell adhesion assay in BE(2)-M17 cells incubated for 24 hr with PTX6 (50–10^4 nM) (average ± SD; N = 3). Results are expressed as percentage of CyQuantGR-induced fluorescence in adherent cells with respect to control (untreated) cells.

which showed no significant differences in total DNA content following 48 hr incubation at 10^2 to 10^4 nM PTX6. Altogether, these results demonstrate that growth inhibition is not a major outcome of PTX6-induced toxicity *in vitro*.

3.4. Effect on cytosolic calcium levels

The effect of PTX6 on cytosolic calcium levels was checked by Fura-2 experiments. PTX6 did not induce any change in cytosolic calcium levels both in a calcium-free or in a calcium-containing medium (data not shown). We checked PTX6 effect on calcium influx induced by intracellular calcium stores depletion. Fig. 7 shows cytosolic calcium levels in human lymphocytes in the presence of PTX6 and thapsigargin (Th). This drug is a tumor-promoting sesquiterpene lactone that inhibits Ca^{2+}-ATPase from intracellular pools [31]. When thapsigargin is added to the cells in a calcium-free medium, a cytosolic calcium increase takes place corresponding to the release from intracellular pools. Then, when calcium is added back to the extracellular medium, an important increase in cytosolic calcium happens due to the entry from extracellular medium, namely capacitative calcium influx [32]. As shown in Fig. 7A, when PTX6 is added after thapsigargin treatment in a Ca^{2+}-free medium, cytosolic calcium is not modified; however, the influx due to calcium readdition is significantly reduced. On the contrary, when PTX6 is added before thapsigargin treatment, both calcium release and calcium influx were increased (Fig. 7B).

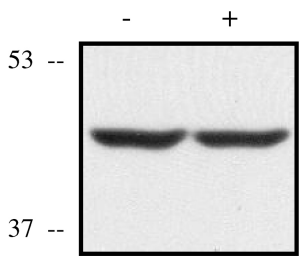

Fig. 3. Effect of PTX6 treatment of BE(2)-M17 cells on immunoreactive actin in cytosoluble extracts. Cells were incubated at 37° for 24 hr with (+) 1 μM PTX6 or vehicle (−), as indicated, before being processed to obtain cytosoluble extracts, which were fractionated by SDS–PAGE and subjected to immunoblotting using anti-actin antibody. The electrophoretic mobilities of fumarase (53 kDa) and lactic dehydrogenase (37 kDa) subunits, used as marker proteins running in a parallel lane, are indicated on the left.

3.5. Effect on cAMP levels

The effect of PTX6 on cAMP cytosolic levels in human lymphocytes is shown in Table 1. In control conditions, that is without any toxin/drug, and after 10 min, the increase in fluorescence dye ratio was 1.57 ± 0.96. In the presence of PTX6 no modifications on cAMP were observed after 10 min incubation, either in a calcium containing medium (1.28 ± 0.36) or after cAMP was increased in the presence of forskolin (3.26 ± 2.16). However, in a calcium-free medium a significant increase in

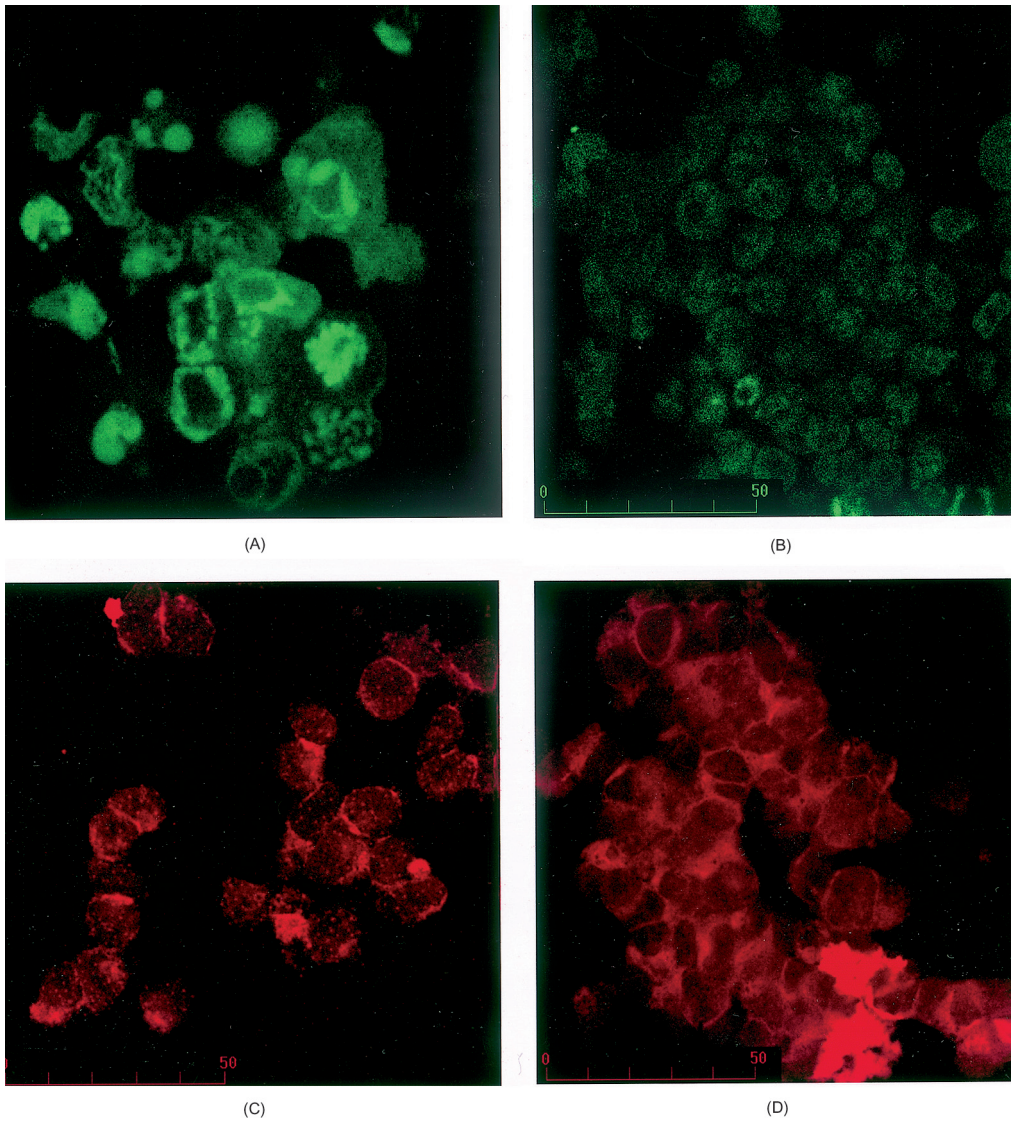

Fig. 4. Fluorescent labeling of F-actin (A, B) and G-actin (C, D) in control (A, C) or PTX6-treated (4, 4) BE(2)-M17 cells. Neuroblastoma cells grown in cell culture slides were exposed to 10^4 nM PTX6 for 24 hr and F-/G-actin were stained as detailed in Section 2. Photographs included are representative of three independent experiments.

fluorescence dye ratio was observed (5.53 ± 0.53) which means an increase in cAMP levels.

4. Discussion

During last years, PTXs have been reported in shellfish from different countries [4–6], thus, gaining an increasing interest for both shellfish producers and Public Health authorities. However, toxicological data on PTXs are still very scarce and its mechanism of action is currently unknown. In this report, we present the first data on cytotoxic activity of PTX6, a member of PTX group isolated from toxic scallops [11]. Results reported in this work provide initial evidence of the mechanism of toxicity and active concentrations of PTX6 in eukaryotic cells.

Table 1
Increase in FlCRhR emission ration (%) after 10 min (control), after 10 min in the presence of 1 μM PTX6 in a Ca^{2+}-containing solution, after 10 min in the presence of 1 μM PTX6 in a Ca^{2+}-free medium, and after 10 min in the presence of 1 μM PTX6 when cAMP were previously increased (9.34 ± 2.09) by 30 μM forskolin preincubation

	Control	PTX6 in Ca^{2+}-containing medium	PTX6 in Ca^{2+}-free medium	PTX6 after cAMP increase
cAMP increases	1.57 ± 0.96	1.28 ± 0.36	5.53 ± 0.53	3.26 ± 2.16

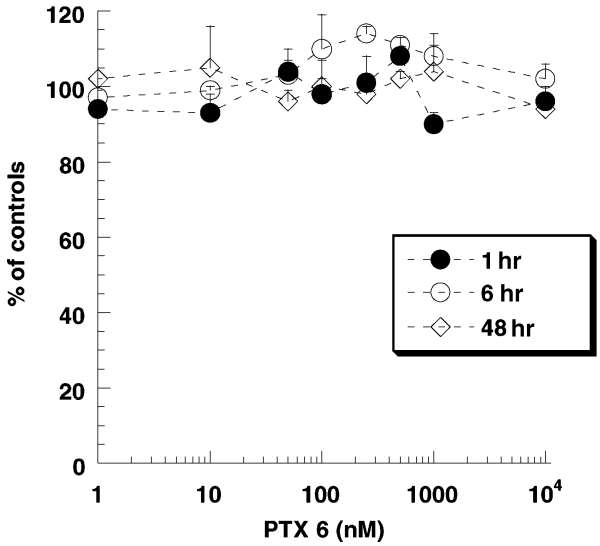

Fig. 5. Changes in mitochondrial membrane potential of BE(2)-M17 cells incubated for 1–48 hr with 1–10^4 nM PTX6 (average ± SD; N = 3). Results are expressed as percentage of Mitotracker® Red CMXRos-retained fluorescence in PTX6-treated cells with respect to controls.

We have demonstrated that F-actin cytoskeleton is a selective target for PTX6 *in vitro*, inducing a time- and dose-dependent change in the polymerization state of actin. These results agree with previous reports [23,28], indicating that the actin cytoskeleton is the target of an increasing number of marine natural drugs which disrupt the organization of F-actin. Furthermore, PTX2 has already been reported to induce a collapse of F-actin bundles in NRK-52E cells following 1 hr exposure at 12.5 nM, which is also accompanied by increased staining of monomeric G-actin [28]. Those results fully agree with our data concerning PTX6, and strongly suggest that different PTX share a common mechanism of action but differ in their relative potency. Indeed, PTX6-induced disruption of F-actin cytoskeleton was observed at higher doses than those reported for PTX2, which agrees with previous data on mouse lethality for these toxins [3,11], thus, also supporting the hypothesis of PTX2 as the parental and most toxic compound of the PTX group.

The specificity of PTX6 causing cytoskeletal changes is also supported by previous observations [8] following intraperitoneal injection of PTXs in mice. That study demonstrated vacuole formation in the liver similar to those caused by phalloidin, a known actin-disrupting cyclic oligopeptide [33]. Furthermore, *in vitro* primary cultures of hepatocytes exposed to PTX1 also showed morphological changes, disruption of stress fibers and accumulation of actin at the cellular peripheries [10], thus, highlighting the role of cytoskeletal changes in the mechanism of toxicity of PTXs.

The actin cytoskeleton can be considered as a highly dynamic structure, and a huge amount of works demonstrate its key role in signal transduction and other regulatory pathways within eukaryotic cells [34]. As mentioned above, the actin cytoskeleton is affected by several marine natural compounds such as okadaic acid [23,35,36], another lipophilic phycotoxin which has been classically included with PTXs in the DSP group. However, F-actin disruption induced by okadaic acid in neuroblastoma cells is accompanied by marked changes which include cell detachment, collapse of mitochondrial membrane potential and, finally, apoptosis [37]. By contrast, results obtained in this work provide evidence that cytoskeletal disruption induced by PTX6 does not involve changes in mitochondrial membrane potential, total DNA content or cell attachment to the ECM. Both decreased DNA levels and loss of

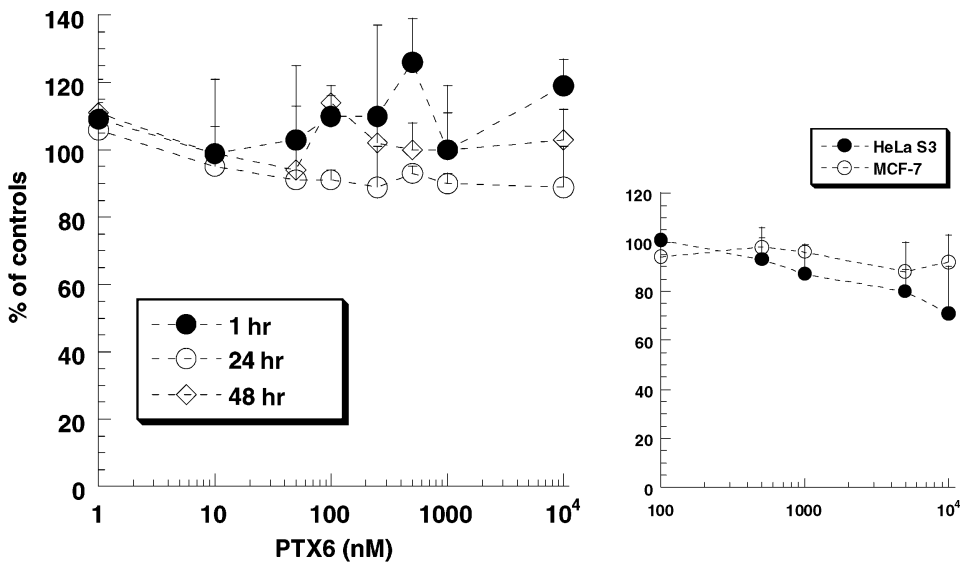

Fig. 6. Effect of PTX6 on cell proliferation rate in eukaryotic cells. BE(2)-M17 or MCF-7/HeLa S3 (inset) cells were exposed to PTX6 for 1–48 hr (BE(2)-M17) or 24 hr (MCF-7; HeLa S3) and total nucleic acids were measured as described in Section 2. Results are expressed as percentage of fluorimetric values obtained with respect to control (untreated) cells.

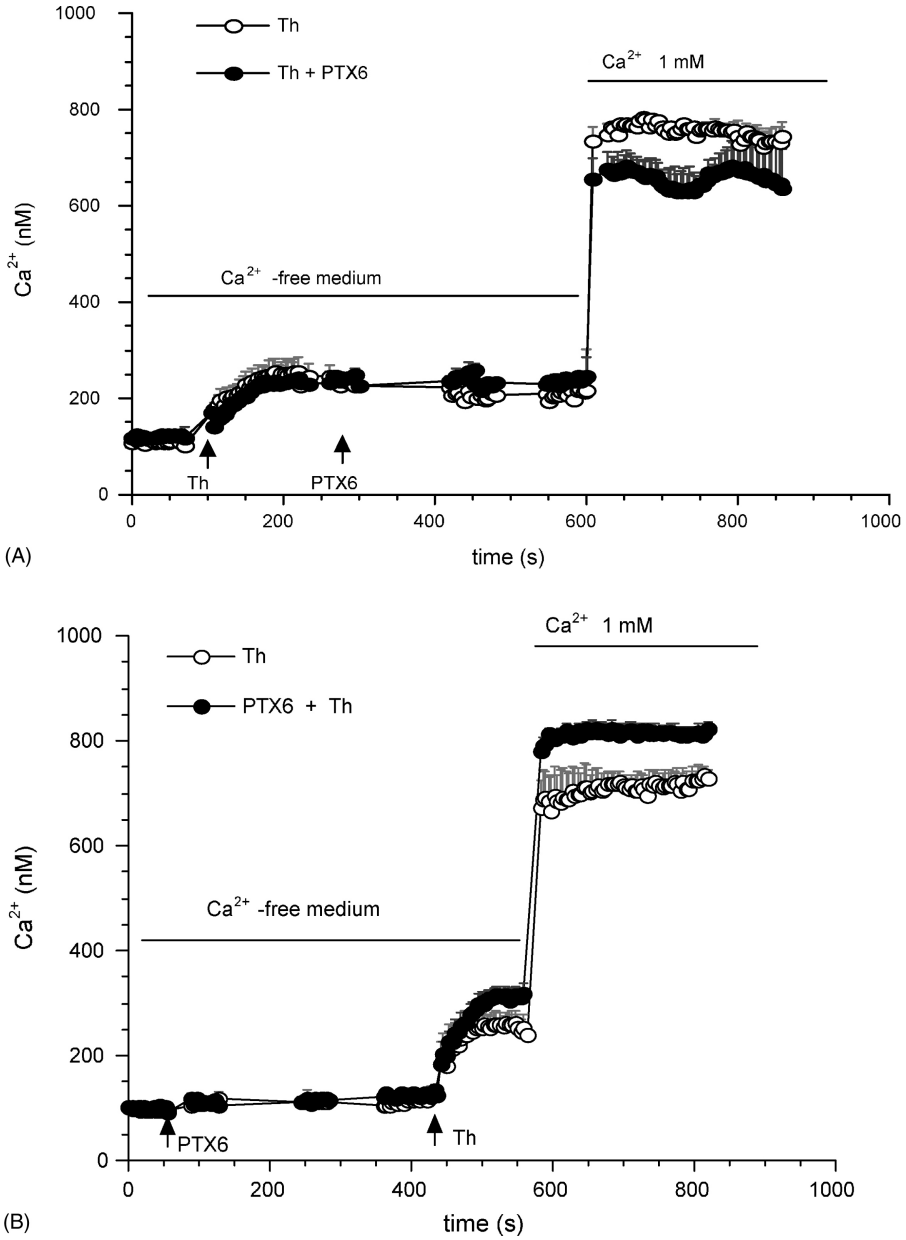

Fig. 7. Effect of PTX6 on cytosolic calcium levels in human lymphocytes in the presence of thapsigargin. Lymphocytes attached to coverslips were bath by a Ca^{2+}-free solution. (A) 0.5 μM thapsigargin was added before 1 μM PTX6. (B) 1 μM PTX6 was added before 0.5 μM thapsigargin.

mitochondrial membrane potential are common events in the execution phase of apoptosis [30,38–41], thus, indicating that apoptosis is not a major outcome of PTX6-induced toxicity *in vitro*. The specificity of cytoskeletal changes in PTX6-treated cells should therefore be considered since no major toxic events have been identified in the cells.

These cytoskeletal changes are accompanied with changes in cytosolic calcium and cAMP. Calcium data show that PTX6 inhibits capacitative calcium influx only when this influx is previously activated, while the toxin alone does not have any direct effect on cytosolic calcium. That is, only when the ionic channel is open the toxin inhibits the entry. The increase in calcium influx observed when PTX6 is added before thapsigargin might be due to a larger pool depletion in the presence of both drugs. Only when calcium is not present in the extracellular medium PTX6 does induce changes in cAMP levels. This effect might be caused by the inhibition of some calcium-dependent phosphodiesterase [42]. Also, the effect in cAMP levels in a calcium-free medium can be caused by the inactivation of some membrane inhibitory mechanism that prevents PTX6 effect on cAMP when calcium is present. In this sense, the regulation of adenyl cyclase, the main mechanism that synthesizes cAMP in cells, can be induced by calcium, even this effect is dependent on cytosolic calcium [43] and, as we show, PTX6 does not modify intracellular calcium levels.

In summary, we conclude that PTX6 exerts its toxic activity through specific disruption of F-actin cytoskeleton, which is not accompanied by other major changes in

neuroblastoma cells. In addition, in human lymphocytes this toxin induces an inhibition of capacitative calcium influx and an increase in cAMP levels. The precise mechanism of PTX6-induced depolymerization of the actin cytoskeleton, as well as downstream signal transduction pathways affected by this toxin should therefore be studied in order to elucidate the molecular basis of its toxicity.

Acknowledgments

This work was funded with grants REN2001-2959-C04-03/MAR and FEDER-CICYT-1FD97-0153 from Ministerio de Ciencia y Tecnología (SPAIN), Xunta Galicia (PGIDT99INN26101 and PGIDT00MAR26101PR), and MCYT(DGI) BMC2000-0441. The authors thank technical assistance of CACTI from Universidad de Vigo (Spain) in the experiments with confocal microscope.

References

[1] Yasumoto T, Murata M, Oshima Y, Matsumoto GK, Clardy J. Diarrhetic shellfish poisoning. American Chemical Society, vol. 262, 1984.
[2] Draisci R, Lucentini L, Mascioni A. Pectenotoxins and yessotoxins: chemistry, toxicology, pharmacology and analysis. New York: Marcel Dekker, 2000.
[3] Sasaki K, Wright JLC, Yasumoto T. The identification and characterization of pectenotoxin (PTX) 4 and PTX7 as spiroketal stereoisomers of two previously reported pectenotoxins. J Org Chem 1998;63: 2475–80.
[4] Draisci R, Lucentini L, Giannetti L, Boria P, Poletti R. First report of pectenotoxin-2 (PTX-2) in algae (*Dinophysis fortii*) related to seafood poisoning in Europe. Toxicon 1996;34:923–35.
[5] Daiguji M, Satake M, James KJ, Bishop A, Mackenzie L, Naoki H, Yasumoto T. Structures of new pectenotoxin analogs, pectenotoxin-2 seco acid and 7-epi-pectenotoxin-2 seco acid, isolated from a dinoflagellate and greenshell mussels. Chem Lett 1998;7:653–4.
[6] James KJ, Bishop AG, Draisci R, Palleschi L, Marchiafava C, Ferretti E, Satake M, Yasumoto T. Liquid chromatographic methods for the isolation and identification of new pectenotoxin-2 analogues from marine phytoplankton and shellfish. J Chromatogr A 1999;844:53–65.
[7] Hamano Y, Kinoshita Y, Yasumoto T. Suckling mice assay for diarrhetic shellfish toxins. In: Anderson DMW, Baden, DG, editors. Toxic dinoflagellates. Amsterdam: Elsevier, 1985. p. 383–8.
[8] Terao K, Ito E, Yanagi T, Yasumoto T. Histopathological studies on experimental marine toxin poisoning. Part I. Ultrastructural changes in the small intestine and liver of suckling mice induced by dinophysistoxin-1 and pectenotoxin-1. Toxicon 1986;24:1141–51.
[9] Aune T, Yasumoto T, Engeland E. Light and scanning electron microscopic studies on effects of marine algal toxins toward freshly prepared hepatocytes. J Toxicol Environ Health 1991;34:1–9.
[10] Zhou ZH, Komiyama M, Terao K, Shimada Y. Effects of pectenotoxin-1 on liver cells *in vitro*. Nat Toxins 1994;2:132–5.
[11] Yasumoto T, Murata M, Lee JS, Torigoe K. Polyether toxins produced by dinoflagellates. In: Natori S, Hashimoto K, Ueno Y, editors. Mycotoxins and phycotoxins. Amsterdam: Elsevier, 1989. p. 375–82.
[12] Nagai H, Satake M, Yasumoto T. Antimicrobial activities of polyether compounds of donoflagellate origins. J Appl Phycol 1990;2:305–8.
[13] Jung JH, Sim CJ, Lee CO. Cytotoxic compounds from a two-sponge association. J Nat Prod 1995;58:1722–6.
[14] Boe R, Gjertsen BT, Vintermyr OK, Houge G, Lanotte M, Doskeland SO. The protein phosphatase inhibitor okadaic acid induces morphological changes typical of apoptosis in mammalian cells. Exp Cell Res 1991;195(1):237–46.
[15] Rossini GP, Pinna C, Viviani R. Inhibitors of phosphoproteoin phosphatases 1 and 2A cause activation of a 53 kDa protein kinase accompanying the apoptotic response of breast cancer cells. FEBS Lett 1997;410:347–50.
[16] Nuydens R, de Jong M, Van Den Kieboom G, Heers C, Dispersyn G, Cornelissen F, Nuyens R, Borgers M, Geerts H. Okadaic acid-induced apoptosis in neuronal cells: evidence for an abortive mitotic attempt. J Neurochem 1998;70(3):1124–33.
[17] Riordan FA, Foroni L, Hoffbrand AV, Mehta AB, Wickremasinghe RG. Okadaic acid-induced apoptosis of HL60 leukemia cells is preceded by destabilization of bcl-2 mRNA and downregulation of bcl-2 protein. FEBS Lett 1998;435(2/3):195–8.
[18] Leira F, Vieites JM, Vieytes MR, Botana LM. Apoptotic events induced by the phosphatase inhibitor okadaic acid in normal human lung fibroblasts. Toxicol In Vitro 2001;15(3):199–208.
[19] Rossini GP, Sgarbi N, Malaguti C. The toxic responses induced by okadaic acid involve processing of multiple caspase isoforms. Toxicon 2001;39:763–70.
[20] Fladmark KE, Serres MH, Larsen NL, Yasumoto T, Aune T, Doskeland SO. Sensitive detection of apoptogenic toxins in suspension cultures of rat and salmon hepatocytes. Toxicon 1998;36:1101–14.
[21] Yasumoto T, Murata M, Lee JS, Torigoe K. Polyether toxins produced by dinoflagellates. In: Natori S, Hashimoto K, Ueno Y, editors. Mycotoxins and phycotoxins, vol. 88. Amsterdam: Elsevier, 1989. p. 375–82.
[22] Sasaki K, Satake M, Yasumoto T. Identification of the absolute configuration of pectenotoxin-6, a polyether macrolide compound, by NMR spectroscopic method using a chiral anisotropic reagent, phenylglycine metho ester. Biosci Biotech Biochem 1997;61(10): 1783–5.
[23] Leira F, Alvarez C, Vieites JM, Vieytes MR, Botana LM. Study of cytoskeletal changes induced by okadaic acid in BE(2)-M17 cells by means of a quantitative fluorimetric microplate assay. Toxicol In Vitro 2001;15:277–83.
[24] Smith PK, Krohn RI, Hermanson GT, Mallia AK, Gartner FH, Provenzano MD, Fujimoto EK, Goeke NM, Olson BJ, Klenk DC. Measurement of protein using bicinchoninic acid. Anal Biochem 1985;150(1):76–85.
[25] Laemmli UK. Cleavage of structural proteins during the assembly of the head of bacteriophage T4. Nature 1970;277:680–5.
[26] Grynkiewicz G, Poenie M, Tsien RY. A new generation of Ca^{2+} indicators with greatly improved fluorescence properties. J Biol Chem 1985;260:3440–50.
[27] Adams SR, Harootunian AT, Buechler YJ, Taylor SS, Tsien RY. Fluorescence ratio imaging of cyclic AMP in single cells. Nature 1991;349:694–7.
[28] Spector I, Braet F, Shochet NR, Bubb MR. New anti-actin drugs in the study of the organization and function of the actin cytoskeleton. Microsc Res Technol 1999;47:18–37.
[29] Gottlieb RA. Mitochondria: execution central. FEBS Lett 2000;482: 6–12.
[30] Hengartner MO. The biochemistry of apoptosis. Nature 2000;407: 770–6.
[31] Thastrup O, Linnebjerg H, Bjerrum PJ, Knudsen JB, Christensen SB. The inflammatory and tumor-promoting sesquiterpene lactone, thapsigargin, activates platelets by selective mobilization of calcium as shown by protein phosphorylations. BBA 1987;927:65–73.
[32] Putney Jr JW. The capacitative model for receptor-activated calcium entry. Adv Pharmacol 1991;22:251–69.
[33] Wieland T. Poisonous principles of mushrooms of the genus *Amanita*. Science 1968;159:946–52.
[34] Salmon ED, Way M. Cytoskeleton. Curr Opin Cell Biol 1999;11:15–7.

[35] Kreienbühl P, Keller H, Niggli V. Protein phosphatase inhibitors okadaic acid and calyculin A alter cell shape and F-actin distribution and inhibit stimulus-dependent increases in cytoskeletal actin of human neutrophils. Blood 1992;80(11):2911–9.
[36] Fiorentini C, Matarrese P, Fattorossi A, Donelli G. Okadaic acid induces changes in the organization of F-actin in intestinal cells. Toxicon 1996;34(8):937–45.
[37] Leira F, Alvarez C, Vieites JM, Vieytes MR, Botana LM. Characterization of distinct apoptotic changes induced by okadaic acid and yessotoxin in the BE(2)-M17 cell line. Toxicol In Vitro 2002;16(1): 23–31.
[38] König K, Liang H, Berns MW, Tromberg BJ. Cell damage by near-IR microbeams. Nature 1995;377(6544):20–1.
[39] Bonfoco E, Leist M, Zhivotovsky B, Orrenius S, Lipton SA, Nicotera P. Cytoskeletal breakdown and apoptosis elicited by NO donors in cerebellar granule cells require NMDA receptor activation. J Neurochem 1996;67(6):2484–93.
[40] Frey T. Correlated flow cytometric analysis of terminal events in apoptosis reveals the absence of some changes in some model systems. Cytometry 1997;28(3):253–63.
[41] Poot M, Gibson LL, Singer VL. Detection of apoptosis in live cells by MitoTracker red CMXRos and SYTO dye flow cytometry. Cytometry 1997;27(4):358–64.
[42] Zhao AZ, Yan C, Sonnenburg WK, Beavo JA. Recent advances in the study of Ca^{2+}/CaM-activated phosphodiesterases-expression and physiological functions. Adv Sec Mess Phosph 1997;31:237–51.
[43] Chiono M, Mahey R, Tate G, Cooper DMF. Capacitative Ca^{2+} entry exclusively inhibits cAMP synthesis in C6-2B glioma cells. Evidence that physiologically evoked Ca^{2+} entry regulates Ca^{2+}-inhibitable adenyl cyclase in non-excitable cells. J Biol Chem 1995;270:1149–55.